



Published in final edited form as:

*NMR Biomed.* 2014 June ; 27(6): 726–732. doi:10.1002/nbm.3114.

## MRI assessment of cerebral oxygen metabolism in cocaine-addicted individuals: Hypoactivity and dose dependence

Peiyong Liu<sup>a,b,\*</sup>, Hanzhang Lu<sup>a,b</sup>, Francesca M. Filbey<sup>c</sup>, Carol A. Tamminga<sup>b</sup>, Yan Cao<sup>d</sup>, and Bryon Adinoff<sup>b,e</sup>

<sup>a</sup>Advanced Imaging Research Center, University of Texas Southwestern Medical Center, Dallas, Texas 75390

<sup>b</sup>Department of Psychiatry, University of Texas Southwestern Medical Center, Dallas, Texas 75390

<sup>c</sup>Center For Brain Health, University of Texas at Dallas, Dallas, Texas 75235

<sup>d</sup>Department of Mathematical Sciences, University of Texas at Dallas, Richardson, Texas 75080

<sup>e</sup>VA North Texas Health Care System, Dallas, Texas 75216

### Abstract

Long-term cocaine use is known to negatively impact neural and cerebrovascular systems. However, the use of imaging markers to separately assess these parameters remains challenging. The primary reason is that most functional imaging markers such as cerebral blood flow, functional connectivity, and task-evoked functional MRI are known to reflect a complex interplay between neural and vascular components, thus the interpretation of the results is not straightforward. The goal of the present study is to examine neural-activity-specific changes in cocaine addiction, using cerebral metabolic rate of oxygen (CMRO<sub>2</sub>) as a surrogate marker of aggregated neural activity. We applied a recently developed CMRO<sub>2</sub> technique in 13 cocaine-addicted subjects and 13 age and gender matched control subjects, and examined the impact of long-term cocaine use on CMRO<sub>2</sub>. Our results showed that CMRO<sub>2</sub> in cocaine-addicted subjects ( $152 \pm 16$   $\mu\text{mol}/100\text{g}/\text{min}$ ) is significantly lower ( $p=0.031$ ) than that in controls ( $169 \pm 20$   $\mu\text{mol}/100\text{g}/\text{min}$ ). Furthermore, the severity of this decreased metabolism is associated with lifetime cocaine use ( $p=0.05$ ). Additionally, the CMRO<sub>2</sub> reduction was accompanied by a trend of decrease in cerebral blood flow ( $p=0.058$ ), but venous oxygenation was unaffected ( $p=0.96$ ), which suggested that the CMRO<sub>2</sub> change may be attributed to a vascular deficiency in chronic cocaine users. To our knowledge, this is the first study to measure CMRO<sub>2</sub> in cocaine addicted individuals. Our findings suggest that CMRO<sub>2</sub> may be a promising approach for assessing the long-term effects of cocaine use on the brain.

### Keywords

cocaine addiction; cerebral metabolic rate of oxygen; MRI; brain functions

---

\*Corresponding Author: Peiyong Liu, PhD, Advanced Imaging Research Center, University of Texas Southwestern Medical Center, 5323 Harry Hines Blvd, Dallas, TX 75390, Tel: 214-645-2806, Fax: 214-645-2885, peiyong.liu@utsouthwestern.edu.

## Introduction

Cocaine is one of the most reinforcing and addictive drugs of abuse. Long-term cocaine consumption has been shown to reduce cognitive function and increase the risk for stroke, suggesting that cocaine use may have a negative impact on both neural and vascular components of the brain (1,2). Imaging techniques that are sensitive to combined effect of neural and vascular deficits, such as cerebral blood flow (CBF) measured by Arterial-Spin-Labeling (ASL) MRI, resting-state functional connectivity MRI (fcMRI), and task-evoked fMRI, have been widely used in studies of cocaine addicted individuals (3-6). However, a common limitation of many of these studies is that it is difficult to precisely interpret these changes, as a reduction in blood flow could be either due to a dysfunction in cerebral vascular system or a lower metabolic demand by the neural tissues. Therefore, a better understanding of pathophysiology associated with cocaine addiction requires the use of imaging techniques that are capable of disentangling the vascular and tissue alterations. The goal of the present study is to specifically examine the tissue metabolic rate in cocaine-addicted individuals using a novel MRI method.

Brain metabolic rate, denoted by cerebral metabolic rate of oxygen (CMRO<sub>2</sub>), represents the amount of oxygen consumed by the brain per unit time and is thought to be a more direct index of the aggregated neural activity, compared to CBF or BOLD measures. However, the *in vivo* measurement of CMRO<sub>2</sub> has proven challenging. For decades, the CMRO<sub>2</sub> measurement has been considered the “niche market” of positron emission tomography (PET), but the PET measurement requires an on-site cyclotron, the injection/infusion/inhalation of <sup>15</sup>O labeled radio tracers, and an arterial line for dynamic blood sampling (7). Other possible techniques, such as <sup>13</sup>C or <sup>17</sup>O nuclear resonance spectroscopy methods (8,9), also involve exogenous tracers and complex procedures. Therefore, there has not been a clinically practical technique to determine this important parameter.

Recently, our laboratory has developed an MRI method that provides a non-invasive (no exogenous agent), fast (<5 min), and reliable (coefficient of variation <4%) estimation of global CMRO<sub>2</sub> on a standard 3T system (10,11). In this method, CMRO<sub>2</sub> is calculated from CBF, arterial oxygenation ( $Y_a$ ) and venous oxygenation ( $Y_v$ ) using the Fick principle of arteriovenous difference, where whole brain CBF was measured by phase-contrast (PC) MRI (12) and  $Y_v$  was measured by a T2-relaxation-under-spin-tagging (TRUST) MRI technique that was developed in our laboratory (13,14). The TRUST technique has been validated in humans against a gold-standard pulse oximetry method (15), and the Phase-contrast MRI has previously also been validated under both *in vitro* and *in vivo* conditions (16,17). This novel CMRO<sub>2</sub> technique has been used to detect CMRO<sub>2</sub> changes in normal aging (18), multiple sclerosis (19), and Alzheimer’s disease (20).

In the present study, we applied this novel technique to examine the impact of long-term cocaine use on brain oxygen metabolism during early abstinence. We sought to answer two questions: 1) Is CMRO<sub>2</sub> in cocaine-addicted patients significantly different from that in healthy controls? 2) Is there a relationship between the duration of cocaine use and CMRO<sub>2</sub>?

## Material and methods

### Participants

Thirteen male cocaine-addicted subjects (age  $46.6 \pm 6.9$  y) and 13 healthy male controls (age  $44.4 \pm 6.0$  y) were studied. The control subjects had no past or present history of substance use disorder. The cocaine-addicted participants had a primary DSM-IV diagnosis of cocaine dependence and cocaine was their lifetime drug of choice. They were hospitalized as soon as possible after their last reported use of cocaine and remained in a structured, residential unit until study completion. Abstinence was verified throughout residential treatment by urine drug screens. The MRI study was performed between 14-28 days following their last cocaine use. The 14-28 day time frame was chosen to avoid the rapid fluctuations in neural activity that occur within the first few days of cocaine abstinence as well as the more gradual changes that may develop with extended abstinence (21). This time frame also allows the dissipation of withdrawal symptoms such as anxiety and sleep disturbance, which are no longer present two weeks after the cessation of cocaine use. The study was approved by the Institutional Review Boards of the University of Texas Southwestern Medical Center and the VA North Texas Health Care System.

### CMRO2 measurement using MRI

The MRI scans were performed on a standard 3T MR scanner (Philips Medical Systems, Best, the Netherlands). CMRO2 of each subject was measured using a method described previously (10,11). Briefly, global CMRO2 (in unit of  $\mu\text{mol O}_2/\text{min}/100\text{g brain tissue}$ ) was quantified based on arteriovenous difference in oxygen content (Fig. 1), i.e.,  $\text{CMRO}_2 = \text{CBF} \times (Y_a - Y_v) \times C_h$ , where CBF is measured by phase-contrast MRI at the feeding arteries of the brain (12),  $Y_a$  is the arterial blood oxygenation assumed to be 98% (22), and  $C_h$  is a constant representing the capacity of blood to carry O2 and was assumed to be  $8.56 \mu\text{mol O}_2/\text{ml blood}$  (23). The most challenging component, venous oxygenation ( $Y_v$ ), is measured by a novel T2-relaxation-under-spin-tagging (TRUST) MRI technique that was recently developed and validated in our laboratory (13,15). TRUST MRI utilizes the spin-tagging principle on the venous side to separate out the pure venous blood signal by subtracting the labeled image from the control image. The venous blood signal is modulated with different T2 weightings using various numbers of flow-insensitive T2-preparation pulses. The monoexponential fitting of the blood signal to the T2-preparation duration (termed effective echo time [eTE]) then gives the T2 value of the venous blood, which is further converted to  $Y_v$  via the well-known relationship between blood T2 and oxygenation (15,24).

The total scan duration of a complete set of CMRO2 measurements was 4.5 min, including an axial 3D time-of-flight angiogram to visualize the feeding arteries of the brain for PC MRI slice positioning (Fig. 2a), a TRUST scan to measure the venous oxygenation at the superior sagittal sinus which is the major draining vein of the brain (Fig. 2b), and four PC MRI scans corresponding to the four feeding arteries of the brain, left internal carotid artery, right internal carotid artery, left vertebral artery (left VA) and right vertebral artery (right VA), respectively (Fig. 2a) (11). The slice positioning and imaging parameters were following the optimized protocols established earlier (11). Specifically, the time-of-flight angiogram was positioned with the top of the slab at the level of the bottom of pons, with the

imaging parameters as follow: TR/TE/flip angle=20 ms /3.45 ms/18°, field of view (FoV)=160×160×70.5 mm<sup>3</sup>, voxel size=1.0×1.0×1.5 mm<sup>3</sup>, number of slices=47, one 60-mm saturation slab positioned above the imaging slab, scan duration=1.4 min. TRUST sequence was positioned to be parallel to anterior-commissure posterior-commissure line with a distance of 20 mm from the sinus confluence, with the following imaging parameters: TR=3000 ms, TI=1200 ms, voxel size=3.44×3.44×5 mm<sup>3</sup>, four eTEs of 0, 40, 80, and 160 ms,  $\tau_{CPMG}$ =10 ms, scan duration=1.2 min. The four PC MRI slices were placed perpendicular to the target vessels at the level of foramen magnum, with the following imaging parameters: single slice, voxel size=0.5×0.5×5 mm<sup>3</sup>, FoV=200×200×5 mm<sup>3</sup>, maximum velocity encoding=80 cm/s, non-gated, 4 averages, scan duration of one PC MRI scan is 0.5 min.

### Data processing

Data processing of TRUST and PC MRI followed methods used previously using custom-written Matlab scripts (10,11). Briefly, for TRUST MRI data, after motion correction and pairwise subtraction between control and labeled images, a preliminary region-of-interest (ROI) was manually drawn to include the superior sagittal sinus, and the top four voxels with the highest intensity within the ROI were chosen for spatial averaging. The averaged venous blood signals for each eTE were then fitted to a monoexponential function to obtain T2. The T2 was in turn converted to  $Y_v$  via a calibration plot obtained by *in vitro* bovine blood experiments. For PC MRI data, a ROI was manually drawn on the magnitude image of each PC MRI scan by tracing the boundary of the targeted artery. The rater was blinded to the subject category prior to ROI drawing. The phase signals, i.e., velocity values, within the mask were summed to yield the blood flow of each artery. We point out that, although this analysis involves subjective delineation of ROIs, previous methodological studies have shown that the inter-rater reliability of the flow results was relatively high with an  $R^2$  of 0.994, which is largely attributed to the high flow velocities in these major arteries (11). The total blood flow of all four feeding arteries was normalized to the brain's parenchyma volume that was estimated from the high resolution T1-weighted magnetization- prepared rapid gradient-echo image using the software FSL (FMRIB Software Library, Oxford University). Specifically, FSL-BET was first applied to perform skull stripping on the T1 image of the brain. Then FSL-FAST was used to segment the brain image into gray matter, white matter and cerebrospinal fluid. The brain's parenchyma volume was given by the sum of gray and white matter volumes, and converted to the weight of the brain by assuming a parenchyma density of 1.06 g/ml (25). Normalizing the total blood flow to the brain's parenchyma volume yields the unit volume CBF (in ml/100g/min) that has accounted for brain volume differences across subjects and groups.

### Statistical analysis

Group comparisons between the cocaine-addicted subjects and healthy controls were conducted. Since distribution of the CMRO2, CBF and  $Y_v$  values within each group were found to be non-Gaussian according to the Kolmogorov-Smirnov test, the group comparisons were conducted using the Mann-Whitney U test. Within the addicted group, linear regression between the years of lifetime cocaine use and CMRO2 was performed after correcting for the effects of normal aging. The age effect was determined by linear

regression of age and CMRO<sub>2</sub> in the control group, assuming the age effect on CMRO<sub>2</sub> is the same for both groups and is independent of the cocaine effect on CMRO<sub>2</sub>. In a separate analysis, multiple regression was performed on data from all 26 subjects, in which CMRO<sub>2</sub> was used as the dependent variable and age and years of cocaine use were independent variables. A potential interaction effect between age and years of cocaine use was also examined by including the interaction term as an additional regressor in the linear model. A *p* value < 0.05 was considered statistically significant. A *p* value between 0.05 and 0.1 was considered a trend of difference.

## Results

There was no significant difference in age (*p*=0.23) and race (*p*=0.42) between the control group and cocaine-addicted group (Table 1). For the cocaine-addicted subjects, the average lifetime use of cocaine was 11.5±7.7 years, ranging from 0.9 to 24.4 years. Six of the cocaine-addicted participants had a co-morbid active diagnosis of alcohol dependence and one participant had co-morbid cannabis and opioid dependence. Ten of the cocaine-addicted subjects were also light (<10 cigarettes/day) or moderate (<25 cigarettes/day) smokers.

The cocaine-addicted participants showed a significantly lower CMRO<sub>2</sub> relative to controls (*p*=0.031, Fig. 3a). This metabolic difference was accompanied by a trend of decrease in CBF (*p*=0.058, Fig. 3b). Venous oxygenation did not differ between the two groups (*p*=0.96, Fig. 3c). Data of individual subjects are shown in Table 2. Gray/white matter volume ratio was comparable between the two groups (1.26±0.08 vs. 1.24±0.15, *p*=0.92). Thus, the lower CMRO<sub>2</sub> in cocaine-addicted subjects cannot be attributed to the possibility that their brain contains more white matter.

Within the cocaine-addicted participants, the dose-response relationship between CMRO<sub>2</sub> and cocaine use was examined by calculating the cross-correlation between years of lifetime cocaine use and CMRO<sub>2</sub>. CMRO<sub>2</sub> negatively correlated with years of lifetime cocaine use (*r*=-0.55, *p*=0.05) (Fig. 3d). That is, the more years of cocaine use, the lower the CMRO<sub>2</sub>. Multiple regression analysis in all subjects using both age and years of cocaine use as regressors confirmed that years of cocaine use was significantly correlated with CMRO<sub>2</sub> (*t*=-2.78, *p*=0.01). No interaction between age and years of cocaine use on CMRO<sub>2</sub> was observed (*t*=-0.67, *p*=0.51).

In the cocaine-addicted group, the six subjects with alcohol dependence did not significantly differ from the non-alcohol-dependent participants in years of lifetime cocaine use (*t*=0.93, *p* = 0.37) or CMRO<sub>2</sub> (*t*=1.08, *p* = 0.30). Group differences (control vs. cocaine-dependent participants) in CMRO<sub>2</sub> persisted when the participant with active cannabis and opiate dependence was excluded (*t*=2.15, *p* = 0.04). Considering cocaine-addicted participants as three subgroups, based upon the intensity of cigarette smoking [none smoker (*n*=3), light (< 10 cigarette/day, *n*=6) and moderate (>10 but < 25 cigarette/day, *n*=4)], yielded no significant difference in CMRO<sub>2</sub> between groups by analysis of variance (*F*=1.74, *p* = 0.23).

## Discussion

The present study examined the effect of long-term cocaine use on CMRO<sub>2</sub> using a non-invasive MRI technique. A significant reduction in global CMRO<sub>2</sub> was observed in cocaine-addicted participants relative to healthy controls and this reduction was significantly correlated with years of cocaine use. These findings suggest that the long-term use of cocaine reduces overall neural activity.

### Pathophysiological considerations

For the control subjects, we obtained the averaged value of 169.06 $\mu$ mol/100g/min, 55.75ml/100g/min, and 61.85% for CMRO<sub>2</sub>, CBF and Y<sub>v</sub>, respectively. In a previous study of normal aging with 232 subjects (18), the CMRO<sub>2</sub>, CBF and Y<sub>v</sub> at the age of 44.4 years was shown to be 170.44 $\mu$ mol/100g/min, 56.15ml/100g/min, and 60.78%, respectively. Therefore, the physiologic values we obtained from the control subjects are consistent with the normal values at this age range.

There exists very limited literature on energy metabolic changes in cocaine-addicted patients. We are not aware of any studies that quantified *oxygen* metabolic rate in this condition. One laboratory has examined *glucose* metabolism in long-term cocaine users previously. Volkow et al. (26) reported a 9% decrease in glucose metabolism in dorsal medial and dorsal lateral prefrontal cortices of cocaine-dependent participants with an average cocaine use of 3.3 years. As these brain regions represent no more than 10% of the whole brain volume, this would translate to a global glucose metabolism reduction of just 1%. Therefore, our observed 9.8% reduction in global CMRO<sub>2</sub> in cocaine-addicted participants suggests that long-term cocaine use might affect the functional integrity of the brain in a broader manner, unrestricted to the fronto-limbic-striatal regions that have been the primary focus of cocaine addiction literature. It is possible that there exist sub-threshold brain regions in the previous studies in which the metabolic deficit did not reach statistical significance. It is also important to note that, from metabolic pathway point of view, oxygen metabolism is expected to provide a more accurate marker for the brain's energy consumption compared to glucose metabolism (27,28). This is because glucose phosphorylation represents an early step in the metabolic pathway and it does not necessarily correlate with the amount of adenosine triphosphate generation (ATP) generated, when for example lactate is produced by the brain or some of the intermediate metabolites are diverted to neurotransmission pathways (29).

Previous studies reported that chronic cocaine users have significant CBF decrease in a few brain regions including frontal, periventricular and temporal-parietal areas (30,31). In our study, the whole-brain CBF in cocaine-addicted patients showed a trend of difference ( $p=0.058$ ) compared to that in healthy controls, but it did not reach significance. This is probably due to the small sample size in our study. The observation that the reduction in CMRO<sub>2</sub> was accompanied by a decrease in CBF in the presence of unaltered oxygen extraction fraction led us to hypothesize that the metabolic reduction may be initiated by cocaine's vasoconstriction effects. Cocaine modulates vascular tone through its effect on calcium channels or monoamine reuptake of smooth muscle cells (32,33). Cocaine could also induce toxicity to vascular endothelium and subsequently impair endothelium-



dependent vasorelaxation, which, in turn, may contribute to vasospasm (34). Chronic hypoperfusion secondary to these effects (35) may suppress neuronal activity and/or cause neuronal toxicity, resulting in an attenuated global CMRO<sub>2</sub>. This process may underlie the increased risk of ischemic stroke associated with cocaine use (32). Although cocaine-induced vasospasm is relatively transient, repeated cocaine-induced attenuation in CMRO<sub>2</sub> may alter the baseline brain activity more permanently. For example, significant cerebral hypoperfusion has been reported in cocaine-addicted patients even after 6 months of abstinence (30). Therefore, whereas cerebral artery vasospasm has been posited as the etiology underlying persistently diminished CBF in individuals chronically exposed to cocaine (32,35), the same process may explain the associated CMRO<sub>2</sub> deficit.

Reduced CMRO<sub>2</sub> is in agreement with previous findings of diminished resting state functional connectivity (rsFC) in brain networks of long-term cocaine users (3). Consistent with our observation that lower CMRO<sub>2</sub> correlates with increased cocaine use, decreased rsFC also correlated with increased lifetime cocaine use (3). Global hypometabolism in cocaine-dependent individuals might also affect global brain functions, such as attention. Attention, which contains a variety of subcomponent processes involving relatively global brain processes, is perhaps the most well-documented deficit in cocaine-dependent individuals (36).

Although the present study has focused on the brain, it is important to point out that blood flow to the brain is also influenced by cardiovascular function of the individual. In particular, cocaine is known to increase heart rate and blood pressure while decreasing myocardial contractility and ejection fraction. Thus, it is possible that reduced CBF observed in this study can be partly attributed to the effect of cocaine on cardiac function. An examination of cardiac output and its relationship with CBF would be useful to provide insight to this question.

### Technical considerations

In this study, CMRO<sub>2</sub> is written in  $\mu\text{mol O}_2$  per 100 gram brain tissue per minute, accounting for brain volume. Thus, the observed group differences in CMRO<sub>2</sub> cannot be explained by brain size difference across participants and groups. Furthermore, the observation that the gray/white matter volume ratio was not significantly different between the groups suggests that the CMRO<sub>2</sub> differences were not simply reflecting cortical atrophy (relative to white matter). A potential confound in the CMRO<sub>2</sub> quantification was our assumption that the arterial oxygen saturation,  $Y_a$ , was 98% for both the healthy control and cocaine-addicted participants. However, cocaine-addicted participants might have a lower  $Y_a$  due to possible complications in their lung function caused by cocaine use (37). We therefore tested the impact of the assumption of  $Y_a$  on our general conclusion, by using a lower  $Y_a$ , e.g. 96%, in our CMRO<sub>2</sub> calculation for the cocaine-addicted participants. It was found that, using the lower  $Y_a$ , the difference between the cocaine addicted group and the controls became more significant ( $p = 0.002$ ). Therefore, the metabolic deficit observed in the present study cannot be attributed to a  $Y_a$  difference between the groups. In fact, the current results may have under-estimated the extent of the deficit.

A methodological strength of the present study is that the CMRO<sub>2</sub> measurement was performed non-invasively without injecting any exogenous tracers or blood sampling. Therefore, the measurement was performed when the participant was awake and under minimal stress, which are important for assessment of functional physiological parameters. Furthermore, this method can be completed within 5 min on a standard 3T system, which are useful features for clinical applicability. Finally, our earlier technical studies have suggested that the test-retest reproducibility of this CMRO<sub>2</sub> technique might be superior to the PET methods (11).

### Limitation

An important limitation of the present CMRO<sub>2</sub> technique is the lack of spatial resolution. Thus, it is unclear whether the diminished CMRO<sub>2</sub> is present throughout the brain or distributed focally in a few brain regions. It is also possible that certain regions may manifest hyperactivity. As technical development of regional CMRO<sub>2</sub> measurement gains sufficient success, it would be important to reproduce these findings in a future study. The present study is also limited by its small sample size. However, the statistical significance shown by the present data suggest that the robustness of the measurement technique may have helped the detection of the group effect in the small sample size. Another limitation is that the nicotine use in the control group does not match that in the cocaine-addicted group. Although there has not been clear evidence that nicotine consumption would affect baseline CMRO<sub>2</sub>, this factor should be considered. Finally, this study lacks the evaluation in females which should be investigated in future work.

### Conclusion

The present study suggests that cocaine results in a reduction in the brain's oxygen metabolism and MRI measure of CMRO<sub>2</sub> provides a sensitive marker in evaluating this deficit. Furthermore, the degree of the metabolic dysfunction appears to be dependent on the length of cocaine use. These findings, if replicated in larger cohorts, may offer an important approach in assessing the neurotoxic effects of cocaine and offer new targets to mitigate the long-term effects of cocaine.

### Acknowledgments

We thank the staff of Homeward Bound, Inc. and the Substance Abuse Team at the Dallas VA Medical Center for their support in the screening and recruitment of study participants.

Funding support: This study was funded by NIH R01 DA023203 (BA), NIH R01 MH084021 (HL), NIH R01 AG042753 (HL), NIH R01 NS067015 (HL), NIH R21 NS078656 (HL) and NIH UL1TR000451.

### References

1. van Holst RJ, Schilt T. Drug-related decrease in neuropsychological functions of abstinent drug users. *Curr Drug Abuse Rev.* 2011; 4(1):42–56. [PubMed: 21466500]
2. Yang S, Salmeron BJ, Ross TJ, Xi ZX, Stein EA, Yang Y. Lower glutamate levels in rostral anterior cingulate of chronic cocaine users - A (1)H-MRS study using TE-averaged PRESS at 3 T with an optimized quantification strategy. *Psychiatry research.* 2009; 174(3):171–176. [PubMed: 19906515]



3. Gu H, Salmeron BJ, Ross TJ, Geng X, Zhan W, Stein EA, Yang Y. Mesocorticolimbic circuits are impaired in chronic cocaine users as demonstrated by resting-state functional connectivity. *Neuroimage*. 2010; 53(2):593–601. [PubMed: 20603217]
4. Rao H, Wang J, Giannetta J, Korczykowski M, Shera D, Avants BB, Gee J, Detre JA, Hurt H. Altered resting cerebral blood flow in adolescents with in utero cocaine exposure revealed by perfusion functional MRI. *Pediatrics*. 2007; 120(5):e1245–1254. [PubMed: 17974718]
5. Kaufman JN, Ross TJ, Stein EA, Garavan H. Cingulate hypoactivity in cocaine users during a GO-NOGO task as revealed by event-related functional magnetic resonance imaging. *J Neurosci*. 2003; 23(21):7839–7843. [PubMed: 12944513]
6. Kilts CD, Schweitzer JB, Quinn CK, Gross RE, Faber TL, Muhammad F, Ely TD, Hoffman JM, Drexler KP. Neural activity related to drug craving in cocaine addiction. *Arch Gen Psychiatry*. 2001; 58(4):334–341. [PubMed: 11296093]
7. Mintun MA, Raichle ME, Martin WR, Herscovitch P. Brain oxygen utilization measured with O-15 radiotracers and positron emission tomography. *J Nucl Med*. 1984; 25(2):177–187. [PubMed: 6610032]
8. Zhu XH, Zhang Y, Tian RX, Lei H, Zhang N, Zhang X, Merkle H, Ugurbil K, Chen W. Development of (17)O NMR approach for fast imaging of cerebral metabolic rate of oxygen in rat brain at high field. *Proc Natl Acad Sci U S A*. 2002; 99(20):13194–13199. [PubMed: 12242341]
9. Hyder F, Chase JR, Behar KL, Mason GF, Siddeek M, Rothman DL, Shulman RG. Increased tricarboxylic acid cycle flux in rat brain during forepaw stimulation detected with 1H[13C]NMR. *Proc Natl Acad Sci U S A*. 1996; 93(15):7612–7617. [PubMed: 8755523]
10. Xu F, Ge Y, Lu H. Noninvasive quantification of whole-brain cerebral metabolic rate of oxygen (CMRO2) by MRI. *Magn Reson Med*. 2009; 62(1):141–148. [PubMed: 19353674]
11. Liu P, Xu F, Lu H. Test-retest reproducibility of a rapid method to measure brain oxygen metabolism. *Magn Reson Med*. 2013; 69(3):675–681. [PubMed: 22517498]
12. Haccke, EM.; Brown, RW.; Thompson, MR.; Venkatesan, R. *Magnetic Resonance Imaging: Physical Principles and Sequence Design*. Wiley-Liss; New York, NY: 1999. MR Angiography and Flow Quantification.
13. Lu H, Ge Y. Quantitative evaluation of oxygenation in venous vessels using T2-Relaxation-Under-Spin-Tagging MRI. *Magn Reson Med*. 2008; 60(2):357–363. [PubMed: 18666116]
14. Xu F, Uh J, Liu P, Lu H. On improving the speed and reliability of T2-relaxation-under-spin-tagging (TRUST) MRI. *Magn Reson Med*. 2012; 68(1):198–204. [PubMed: 22127845]
15. Lu H, Xu F, Grgac K, Liu P, Qin Q, van Zijl P. Calibration and validation of TRUST MRI for the estimation of cerebral blood oxygenation. *Magn Reson Med*. 2012; 67(1):42–49. [PubMed: 21590721]
16. Evans AJ, Iwai F, Grist TA, Sostman HD, Hedlund LW, Spritzer CE, Negro-Vilar R, Beam CA, Pelc NJ. Magnetic resonance imaging of blood flow with a phase subtraction technique. In vitro and in vivo validation. *Invest Radiol*. 1993; 28(2):109–115. [PubMed: 8444566]
17. Zananiri FV, Jackson PC, Goddard PR, Davies ER, Wells PN. An evaluation of the accuracy of flow measurements using magnetic resonance imaging (MRI). *Journal of medical engineering & technology*. 1991; 15(4-5):170–176. [PubMed: 1800748]
18. Lu H, Xu F, Rodrigue KM, Kennedy KM, Cheng Y, Flicker B, Hebrank AC, Uh J, Park DC. Alterations in cerebral metabolic rate and blood supply across the adult lifespan. *Cereb Cortex*. 2011; 21(6):1426–1434. [PubMed: 21051551]
19. Ge Y, Zhang Z, Lu H, Tang L, Jaggi H, Herbert J, Babb JS, Rusinek H, Grossman RI. Characterizing brain oxygen metabolism in patients with multiple sclerosis with T2-relaxation-under-spin-tagging MRI. *J Cereb Blood Flow Metab*. 2012; 32(3):403–412. [PubMed: 22252237]
20. Thomas, BP.; Sheng, M.; Tseng, B.; Liu, P.; Martin-Cook, K.; Cullum, M.; Weiner, M.; Levine, B.; Zhang, R.; Lu, H. Characterization of CMRO2, resting CBF, and cerebrovascular reactivity in patients with very early stage of Alzheimer's Disease. *Proceedings of the 21st Annual Meeting ISMRM; Salt Lake City, USA*. 2013. p. 619
21. Weddington WW, Brown BS, Haerten CA, Cone EJ, Dax EM, Herning RI, Michaelson BS. Changes in mood, craving, and sleep during short-term abstinence reported by male cocaine

- addicts. A controlled, residential study. *Arch Gen Psychiatry*. 1990; 47(9):861–868. [PubMed: 2393345]
22. West, JB. *Pulmonary physiology and pathophysiology: an integrated, case-based approach*. 2. Philadelphia, PA: Lippincott Williams & Wilkins; 2007.
  23. Guyton, AC.; Hall, JE. *Respiration*. In: Guyton, AC.; Hall, JE., editors. *Textbook of medical physiology*. Saunders/Elsevier; Philadelphia: 2005.
  24. Golay X, Silvennoinen MJ, Zhou J, Clingman CS, Kauppinen RA, Pekar JJ, van Zij PC. Measurement of tissue oxygen extraction ratios from venous blood T(2): increased precision and validation of principle. *Magn Reson Med*. 2001; 46(2):282–291. [PubMed: 11477631]
  25. Herscovitch P, Raichle ME. What is the correct value for the brain–blood partition coefficient for water? *J Cereb Blood Flow Metab*. 1985; 5(1):65–69. [PubMed: 3871783]
  26. Volkow ND, Hitzemann R, Wang GJ, Fowler JS, Wolf AP, Dewey SL, Handlesman L. Long-term frontal brain metabolic changes in cocaine abusers. *Synapse*. 1992; 11(3):184–190. [PubMed: 1636149]
  27. Hyder, F. Deriving Changes in CMRO<sub>2</sub> from Calibrated fMRI. In: Shulman, RG.; Rothman, DL., editors. *Brain Energetics and Neuronal Activity: Applications to fMRI and Medicine*. John Wiley & Sons; 2005.
  28. Baron JC, Rougemont D, Soussaline F, Bustany P, Crouzel C, Bousser MG, Comar D. Local interrelationships of cerebral oxygen consumption and glucose utilization in normal subjects and in ischemic stroke patients: a positron tomography study. *J Cereb Blood Flow Metab*. 1984; 4(2): 140–149. [PubMed: 6609928]
  29. Belanger M, Allaman I, Magistretti PJ. Brain energy metabolism: focus on astrocyte-neuron metabolic cooperation. *Cell metabolism*. 2011; 14(6):724–738. [PubMed: 22152301]
  30. Strickland TL, Mena I, Villanueva-Meyer J, Miller BL, Cummings J, Mehringer CM, Satz P, Myers H. Cerebral perfusion and neuropsychological consequences of chronic cocaine use. *J Neuropsychiatry Clin Neurosci*. 1993; 5(4):419–427. [PubMed: 8286941]
  31. Volkow ND, Mullani N, Gould KL, Adler S, Krajewski K. Cerebral blood flow in chronic cocaine users: a study with positron emission tomography. *Br J Psychiatry*. 1988; 152:641–648. [PubMed: 3262397]
  32. Johnson BA, Devous MD Sr, Ruiz P, Ait-Daoud N. Treatment advances for cocaine-induced ischemic stroke: focus on dihydropyridine-class calcium channel antagonists. *Am J Psychiatry*. 2001; 158(8):1191–1198. [PubMed: 11481148]
  33. Madden JA, Konkol RJ, Keller PA, Alvarez TA. Cocaine and benzoylecgonine constrict cerebral arteries by different mechanisms. *Life Sci*. 1995; 56(9):679–686. [PubMed: 7869849]
  34. Havranek EP, Nademanee K, Grayburn PA, Eichhorn EJ. Endothelium-dependent vasorelaxation is impaired in cocaine arteriopathy. *J Am Coll Cardiol*. 1996; 28(5):1168–1174. [PubMed: 8890811]
  35. Kaufman MJ, Levin JM, Ross MH, Lange N, Rose SL, Kukes TJ, Mendelson JH, Lukas SE, Cohen BM, Renshaw PF. Cocaine-induced cerebral vasoconstriction detected in humans with magnetic resonance angiography. *JAMA*. 1998; 279(5):376–380. [PubMed: 9459471]
  36. Jovanovski D, Erb S, Zakzanis KK. Neurocognitive deficits in cocaine users: a quantitative review of the evidence. *J Clin Exp Neuropsychol*. 2005; 27(2):189–204. [PubMed: 15903150]
  37. Haim DY, Lippmann ML, Goldberg SK, Walkenstein MD. The pulmonary complications of crack cocaine. A comprehensive review. *Chest*. 1995; 107(1):233–240. [PubMed: 7813284]

## Abbreviation used

<b>CMRO<sub>2</sub></b>	cerebral metabolic rate of oxygen
<b>CBF</b>	cerebral blood flow
<b>ASL</b>	Arterial-Spin-Labeling
<b>fcMRI</b>	functional connectivity MRI

<b>PET</b>	positron emission tomography
<b>PC</b>	phase-contrast
<b>TRUST</b>	T2-relaxation-under-spin-tagging
<b>eTE</b>	effective echo time
<b>FOV</b>	field of view
<b>TR</b>	time of repetition
<b>TE</b>	echo time
<b>TI</b>	time of inversion
<b>ICA</b>	internal carotid artery
<b>VA</b>	vertebral artery
<b>ROI</b>	region-of-interest
<b>SD</b>	standard deviation
<b>ATP</b>	adenosine triphosphate generation
<b>rsFC</b>	resting state functional connectivity

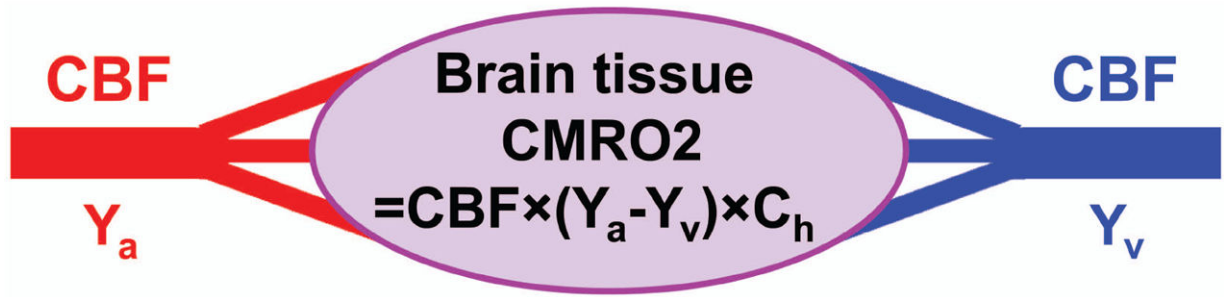


**Fig. 1.**

Illustration of the relationship among different physiologic parameters associated with oxygen demand and supply of the brain. Arterial blood (oxygenation  $Y_a$ ) delivers oxygen to brain tissue, the flow rate of which is denoted by CBF. Brain tissue extracts a portion of the oxygen carried by the blood for its metabolism, the rate of which is denoted by CMRO2. The portion of oxygen that remains in the blood will determine the value of  $Y_v$  and is drained through veins at the rate of CBF.  $C_h$  is a constant representing the oxygen-carrying capacity of blood.

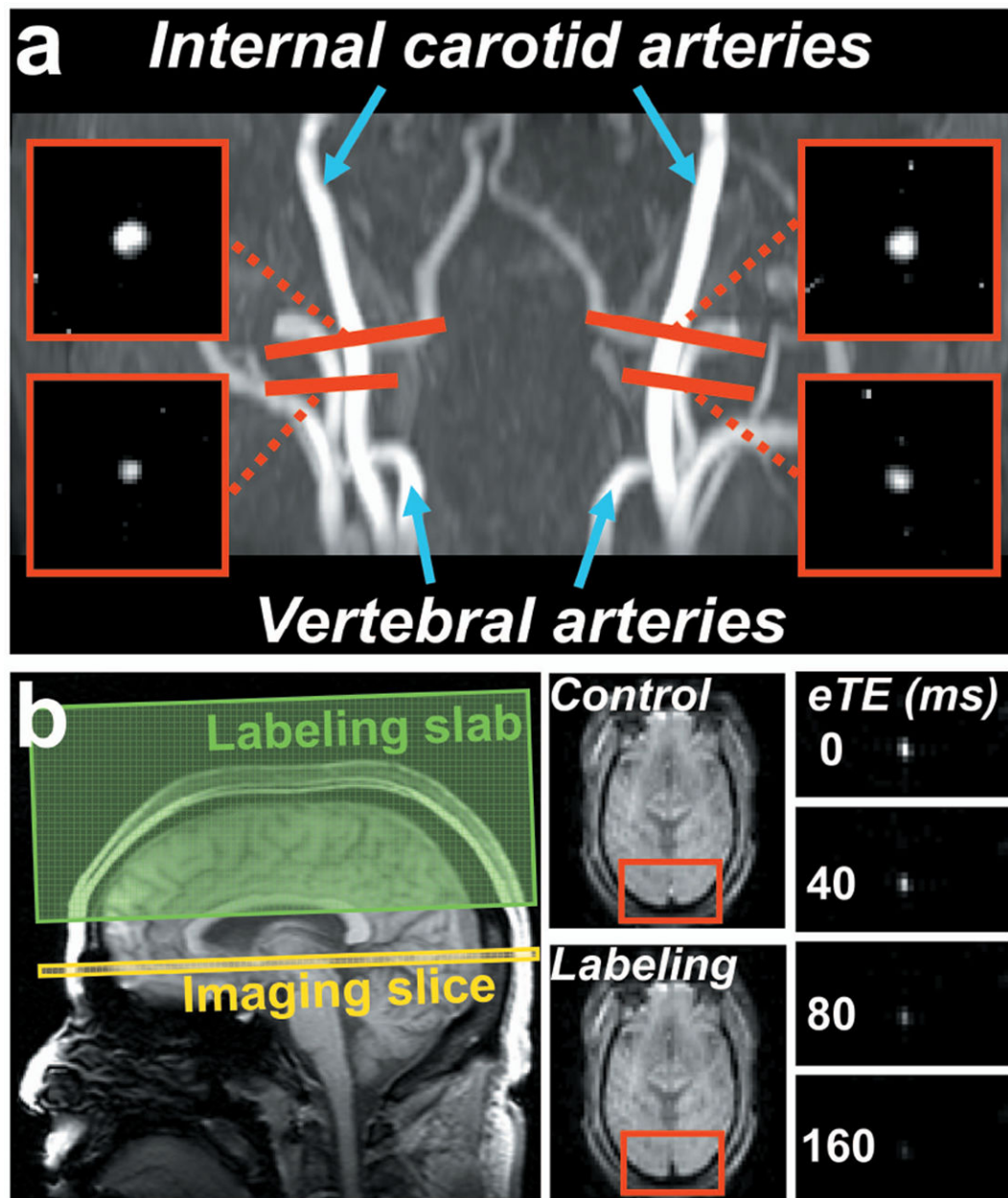


**Fig. 2.** MR images of the CMRO<sub>2</sub> measurement from a representative subject. (a) Positioning and the resulted phase-contrast (PC) images of the four feeding arteries of the brain, i.e., left and right internal carotid arteries, and left and right vertebral arteries. The four PC MRI scans (red bars) are positioned perpendicular to the respective feeding arteries. (b) Positioning and the resulted TRUST images. The imaging slice (yellow box) was positioned to be perpendicular to the superior sagittal sinus. The TRUST technique utilizes the spin-tagging principle with the labeling slab (green box) on the venous side (above the imaging slice). Subtraction of the control and labeled images yields pure blood signal in sagittal sinus, which is then subject to increasing T<sub>2</sub> weightings. The monoexponential fitting of the blood signal to the T<sub>2</sub>-preparation duration (termed effective echo time [eTE]) then gives the T<sub>2</sub>

value of the venous blood. As blood T2 has a well-known relationship with the oxygenation level of the blood, the estimated venous T2 can be converted to  $Y_v$ .



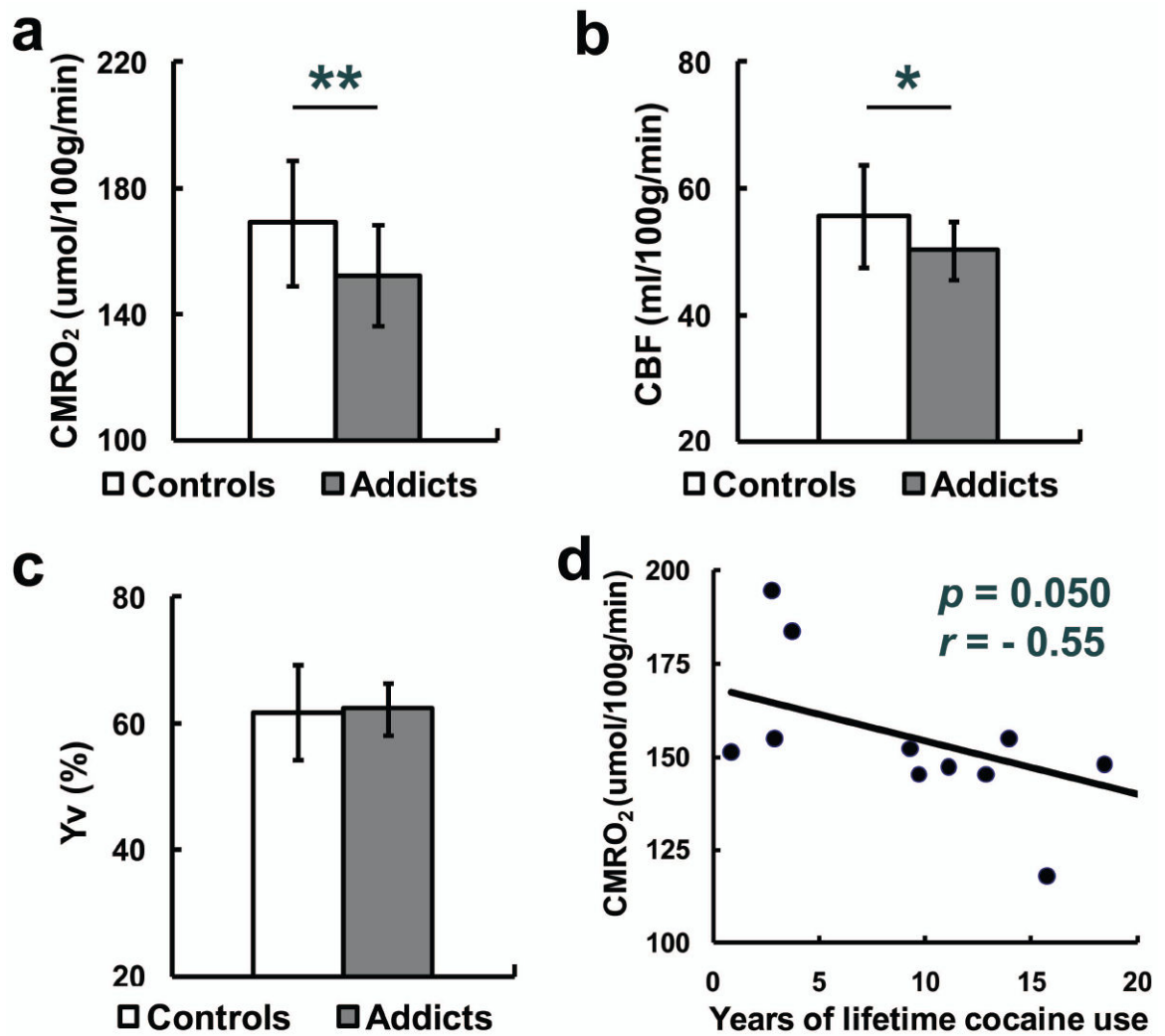


**Fig. 3.** CMRO<sub>2</sub> (mean±SD) (a), CBF (b) and Y<sub>v</sub> (c) in healthy control and cocaine-addicted participants. N = 13 in both groups. Two asterisks indicate significant difference between the two groups ( $p < 0.05$ ), and one single asterisk indicates a trend of difference ( $0.05 < p < 0.1$ ). (d) CMRO<sub>2</sub> and years of lifetime cocaine use in cocaine-addicted participants.

**Table 1**

Demographic characteristics of control and cocaine-addicted participants.

Characteristic	Control (N=13)	Cocaine addicted (N=13)
Age, mean±SD (years)	44.4±6.0	46.6±6.9
Age, range (years)	33-53	30-54
Number of men	13	13
Race		
Black	8	10
White	5	3
Cocaine		
Lifetime cocaine use, mean±SD (years)	--	11.5±7.7
Nicotine Use		
Number of smokers	0	10
Cigarettes/day, mean±SD	--	11.2±8.1 (N=10)
Lifetime cigarettes use (years)	--	14.2±13.1 (N=10)
Alcohol Dependence Disorder	--	6
Cannabis Dependence Disorder	--	1
Opioid Dependence Disorder	--	1

Table 2

CMRO2 data of all participants.

Subject number	Age (Years)	Cocaine use (Years)	Total Blood Flow (ml/min)	CBF (ml/100g/min)	Yv (%)	CMRO2 (μmol/100g/min)
C1	38	--	919.03	71.74	71	165.85
C2	39	--	809.99	63.12	70	151.33
C3	43	--	589.22	51.32	58	175.75
C4	46	--	774.98	63.27	71	146.26
C5	53	--	619.82	55.52	60	180.63
C6	39	--	695.14	50.56	66	138.52
C7	47	--	713.10	55.54	64	161.68
C8	46	--	898.81	64.05	69	159.05
C9	48	--	787.52	58.37	56	209.92
C10	51	--	523.03	43.91	48	187.97
C11	52	--	568.31	46.40	54	174.79
C12	33	--	629.27	48.84	54	190.31
C13	42	--	736.39	51.97	63	155.75
mean±SD	44.4±6.0	--	712.66±124.06	55.74±8.06	61.85±7.50	169.06±20.00
P1	48	9.71	618.69	50.40	64	146.71
P2	53	15.76	481.10	46.63	67	123.78
P3	30	3.74	721.10	57.88	64	168.51
P4	50	23.29	578.79	51.17	68	131.45
P5	54	12.90	636.07	49.41	62	152.31
P6	49	18.46	661.97	54.85	66	150.28
P7	48	24.37	604.01	48.65	60	158.30
P8	49	11.11	582.13	43.71	58	149.70
P9	47	2.93	509.03	43.20	56	155.34
P10	36	9.29	687.04	53.68	67	142.49
P11	51	0.87	625.62	45.37	58	155.38
P12	50	13.94	685.91	54.38	64	158.30
P13	41	2.77	719.28	53.96	57	189.41
mean±SD	46.6±6.9	11.5±7.7	623.90±74.03	50.25±4.61	62.38±4.17	152.46±16.12

Subject number	Age (Years)	Cocaine use (Years)	Total Blood Flow (ml/min)	CBF (ml/100g/min)	Yv (%)	CMRO2 ( $\mu$ mol/100g/min)
P	0.23	--	0.065	0.058	0.96	0.031

C indicates control subjects, P indicates cocaine-addicted subjects.